High-resolution cloud motion analysis with Meteosat-6 Rapid Scans, MISR and ASTER

HIGH-RESOLUTION CLOUD MOTION ANALYSIS WITH METEOSAT-6 RAPID SCANS, MISR AND ASTER

Gabriela SEIZ [1, 2], Manos BALTSAVIAS [1], Armin GRUEN [1]

[1] Institute of Geodesy and Photogrammetry, ETHZ, CH-8093 Zuerich
[2] MeteoSwiss, Kraehbuehlstrasse 58, CH-8044 Zuerich

ABSTRACT

In this study, coincident images of Meteosat-6, MISR (on EOS Terra) and ASTER (on EOS Terra) are used to analyze the cloud motion field in high temporal and spatial resolution.
The Multi-angle Imaging SpectroRadiometer (MISR) has nine cameras at different viewing angles, -70.5° (named DA), -60.0° (CA), -45.6° (BA), -26.1° (AA), 0.0° (AN), 26.1° (AF), 45.6° (BF), 60.0° (CF), and 70.5° (DF), and a spatial resolution of 275 m. The time delay between the MISR camera views is 40-55 s, resulting in a total time span of about 7 minutes between DF and DA. The Advanced Spaceborne Thermal Emission and Reflection Radiometer (ASTER) VNIR subsystem provides nadir and backward looking stereo images of channel 3 (870 nm), with a spatial resolution of 15 m. The stereo configuration is given with the setting angle of 27.6° between the nadir and the backward telescope. The ASTER nadir view (3N) is simultaneously acquired with the MISR AN view, while the backward view (3B) is taken about 55 s later. In the presented case study, the coincident images from the three sensors allow a precise characterization of the cloud motion field on different spatial scales. The stereo matching and tracking is done with a cloud-adapted least-squares matching (LSM) algorithm, developed at our Institute. The retrieved cloud motion winds (CTW) from the Meteosat-6 10-minute Rapid Scans have an accuracy of 2 m/s in East-West direction and an accuracy of 3 m/s in North-South direction; the MISR CTWs have a cross-track accuracy of about 2 m/s and an across-track accuracy of 5-6 m/s and the ASTER cross-track winds can be retrieved with an accuracy of 0.5 m/s.
This study shows that the Meteosat-6 10-minute Rapid Scan Service is an important component for the comparison of cloud motion products from geostationary and polar-orbiting satellites; in the near future, the MSG 15-minute Scans will further increase the comparison and validation possibilities of cloud motion winds over Europe.

1. INTRODUCTION

Meteosat-6 Rapid Scans are an important component to characterize the cloud motion field with a high temporal resolution. In addition to the Meteosat-7 winds, operational motion vector products are now derived with Meteosat-6 Rapid Scan data by EUMETSAT (de Smet, 2002). MSG data will further improve the geostationary cloud motion retrieval possibilities with its 15-minute scans (Rattenborg, 2000). Two developments from polar-orbiting platforms are important to be mentioned, especially for higher latitude regions: 1) the simultaneous cloud-top height and motion retrieval with stereo-photogrammetric methods from the nine viewing angles of MISR onboard EOS-Terra (Horvath and Davies, 2001; Horvath et al., 2002), and 2) the retrieval of cloud and water vapor winds from MODIS onboard EOS-Terra and -Aqua for polar regions (Key et al., 2003).

This paper extends the stereo cloud-top height and motion retrievals described in Seiz and Baltsavias (2000) and Seiz et al. (2001) to multiple views of MISR and to ASTER, with special focus on the motion retrieval. After a description of the data and algorithms, the theoretical accuracies of the cloud motion components are opposed to the results of a case study over Switzerland in April 2002, with coincident images of Meteosat-6, MISR and ASTER. Our cloud-top height/ motion results in high spatial resolution can finally help in the validation of operational cloud motion vector products as it is well recognized today that geometric height techniques (e.g. multi-view photogrammetry) should be used for an independent verification of heights assigned by temperature methods.

2. DATA

2.1 Meteosat-6 Rapid Scans

Following the success of the 5-minute Rapid Scanning support provided to the Mesoscale Alpine Programme (MAP) in Autumn 1999, new 10-minute Rapid Scans were started by EUMETSAT in August 2000 (EUMETSAT, 2003). These trials had normally a duration of 48 to 72 hours a week. Since September 2001, an operational 10-minute Rapid Scanning Service (RSS) is maintained. For the rapid scans, the in-orbit stand-by Meteosat-6 instrument, positioned at 10° W, is used. The limited scan consists of 5000 x 1666 pixels (or 2500 x 833 for IR/WV), starts at line 3171 (or line 1586 for IR/WV) of the operational Meteosat-7 scan and covers an area approximately from 10° to 70° N.

2.2 MISR

The Multi-angle Imaging SpectroRadiometer (MISR) was launched onboard the EOS AM-1 Terra spacecraft in December 1999 (MISR, 2003). The orbit is sun-synchronous at a mean height of 705 km, with an inclination of 98.5° and an equatorial crossing time at about 10:30 am. The repeat cycle is 16 days. The MISR instrument consists of nine pushbroom cameras at different viewing angles: -70.5° (named DA), -60.0° (CA), -45.6° (BA), -26.1° (AA), 0.0° (AN), 26.1° (AF), 45.6° (BF), 60.0° (CF), and 70.5° (DF). The time delay between adjacent camera views is 45-60 seconds which results in a total delay between the DA and DF image of about 7 minutes. The four MISR spectral bands are centered at 446 (blue), 558 (green), 672 (red), and 866 nm (NIR). The data of the red band from all nine cameras and of the blue, green and NIR bands of the AN camera are saved in high-resolution, with a pixel size of 275 x 275 m; the data of the blue, green and NIR bands of the remaining eight cameras are stored in low-resolution, with a pixel size of 1.1 x 1.1 km. The operational data products from NASA are described in Lewicki et al. (1999); the two products used for our investigations are the L1B2 Ellipsoid data (geolocated product) and the L2TC data (top-of-the-atmosphere/ cloud product).

2.3 ASTER

The Advanced Spaceborne Thermal Emission and Reflection Radiometer (ASTER) is an advanced multispectral imager that was launched onboard the EOS AM-1 Terra spacecraft in December 1999, as MISR described above (ASTER, 2003). ASTER covers a wide spectral region with 14 bands from the visible to the thermal infrared with high spatial, spectral and radiometric resolution. An additional backward-looking near infrared band provides stereo coverage. The sensor consists of three separate instrument subsystems: the Visible and Near Infrared (VNIR) has three bands with a spatial resolution of 15 m (named 1, 2, 3N), and an additional backward telescope for stereo (named 3B); the Shortwave Infrared (SWIR) has 6 bands with a spatial resolution of 30 m; and the Thermal Infrared (TIR) has 5 bands with a spatial resolution of 90 m. Each ASTER scene covers an area of 60 km x 60 km.
The VNIR subsystem, which provides the used 3N/3B stereo images, consists of two independent telescope assemblies to minimize image distortion in the backward and nadir looking telescopes. The detectors for each of the bands consist of 5000 element silicon charge coupled detectors. Only 4000 of these detectors are used at any one time. A time lag of about 55 seconds occurs between the acquisition of the nadir and backward image. The stereo configuration is given with the setting angle of 27.60° between the nadir and backward telescopes. The used ASTER Level 1B data are Level 1A data with the radiometric and geometric coefficients applied.

3. METHODS

Matching of near-simultaneous views from a multi-view polar-orbiting instrument (e.g. MISR, ASTER) and tracking of geostationary rapid scans (≤ 10-minute interval) require a similar processing. For both tasks, we apply the Multi-Photo Geometrically Constrained (MPGC) Matching algorithm developed at our Institute (Baltsavias, 1991), which is based on Least-Squares-Matching (LSM) (Grün, 1985). The algorithm has already been tested on a number of ground-based multi-view CCD images of clouds as well as on satellite-based cloud images from ATSR2, MISR and ASTER (Seiz, 2003).

3.1 Matching (MISR, ASTER)

Figure 1 illustrates the processing steps to derive CTH and CTW from MISR and ASTER. As no a priori values of the cloud heights were given to the matching algorithm, a hierarchical matching procedure with 4 pyramid levels for MISR and 7 pyramid levels for ASTER was applied so that the maximum possible parallax at the highest level is only 2-3 pixels. Every pyramid level was enhanced and radiometrically equalized with a Wallis filter (Wallis, 1976). Points with good texture were then selected with an interest operator (Förstner and Gülch, 1987). After the MPGC matching, the matching solutions were quality-controlled with absolute and relative tests on the matching statistics. The resulting y-parallaxes were converted into preliminary cloud heights after Prata and Turner (1997), considering that the zenith angles have to be projected on the along-track plane. From the x-parallaxes, the cross-track motion component was computed. For the final cloud-top heights, the preliminary heights were then corrected by the along-track motion error, with the along-track motion component from Meteosat-6. For MISR triplets (BF-AN-DF, with BF as template image), the final cloud heights, along- and cross-track motion components were additionally calculated with the linear equations described in Diner et al. (1999) and Horvath and Davies (2001). For visualization, the height and motion values of the successfully matched points are finally interpolated with triangulation to a regular grid.

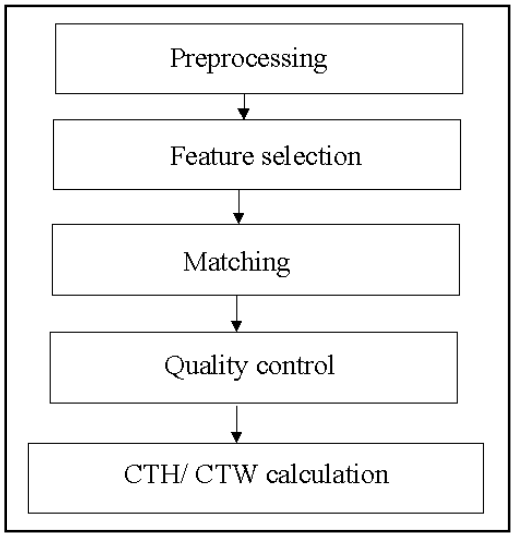

Figure 1. Overview of the processing steps.

3.2 Tracking (Meteosat-6)

Before tracking, the images were preprocessed with a Wallis filter for contrast enhancement. The corresponding points in the image sequence were then determined with the MPGC matching algorithm. Because of the larger disparities (up to about 10 pixels) compared with the 5-minute MAP Rapid Scans, two pyramid levels (original + 1st pyramid level) were used in the matching. Blunders are excluded in the quality control step with absolute and relative tests on the matching statistics. As the features – even clouds – are very self-similar within these 10 minutes, the tracking of cloud points is much easier compared to tracking of the operational 30-minute Meteosat-7 series where it can be difficult to select good cloud tracers (Schmetz et al., 1993).

3.3 Theoretical cloud motion retrieval accuracies

The accuracy of the retrieved cloud-top heights and winds with stereo-photogrammetric methods is largely influenced by the geometric configuration (base-to-height ratio B/H, time difference Δt) and by the matching accuracy. The MPGC LSM matching algorithm is well known for its high accuracy and reliability. In the case of clouds, the theoretical accuracy σ of the matching is about $\pm$ 0.5 pixels, which is of course worse than for e.g. signalized points. Table 1 summarizes the estimated accuracies of the along- and cross-track motion components for the three instruments and different retrieval methods. It is important to note that these theoretical accuracies only include the geometric configuration and the matching accuracy, but no systematic errors which could occur (e.g. geolocation errors, angle/time errors, etc.).

Sensor	Pixel size [m]	B/H	Δt [s]	Cross-track motion accuracy σ (u') [m/s]	Along-track motion accuracy σ (v') [m/s]
ASTER	15	0.60	55	0.2	-
MISR AN_AF	275	0.49	46	3.0	-
MISR BF_AN_DF		1.02; 1.83	91; 112	1.5	5.6
Meteosat-6	2500 x 4000	-	600	2.0	3.0

Table 1. Theoretical accuracies of the cloud motion retrieval from ASTER, MISR AN_AF, MISR BF_AN_DF and Meteosat-6 Rapid Scans.

4. RESULTS

All the above described methods were applied to a dataset in April 2002 with coincident images of MISR, ASTER and Meteosat-6. Table 2 shows the exact acquisition periods of the three satellite systems.

Sensor	Acquisition time (at 47° N)	Frequency
MISR (block 52)	DF: 10:31:36, …, AN: 10:35:02, …, DA: 10:38:28	16 days
ASTER	3N: 10:35:03, 3B: 10:35:58	16 days (on demand only)
Meteosat-6	10:27:21/ 10:37:21/ 10:47:21/ ...	10 min

Table 2. Acquisition times (UTC) of MISR, ASTER and Meteosat-6 data on 12/04/2002.

Optimally, all nine viewing angles of MISR should be analyzed simultaneously. However, due to cloud motion and due to different viewing angles, the identification of cloud points through more than 2-3 views is difficult, as illustrated in Figure 2. In this study, we worked on the AN-AF stereo pair and on the BF-AN-DF triplet. For the triplet, the center view of the three views, BF, was chosen as template image. The approximate positions in the AN and DF image were then extrapolated from the AN-AF matching results.

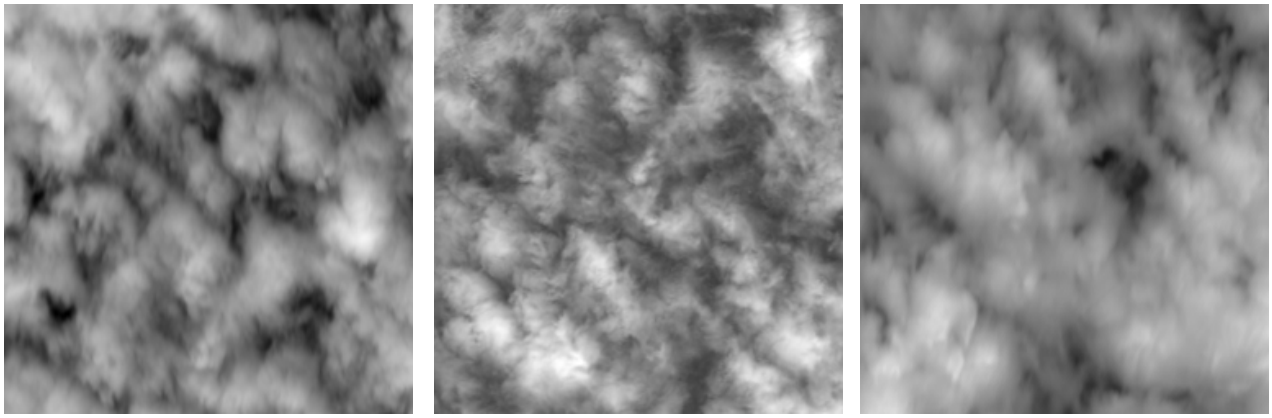

Figure 2. Cloud field during 7-minute interval from MISR DF (left) to MISR AN (center) to MISR DA view.

As ASTER is mounted on the same satellite as MISR, this offers the unique possibility to analyze clouds both on 275 m and 15 m spatial resolution. Figure 3 illustrates which new cloud structure details are visible in the ASTER image compared with the MISR image. The non-continuous data acquisition and the small FOV of ASTER (60 km swath width) do not allow to use this sensor for operational cloud height and motion retrievals, but it is a valuable data source for local validation studies. The correction of the motion error in the ASTER stereo cloud-top heights had to be done with external cloud motion information (as ASTER has only one nadir and one backward view), either derived from Meteosat-6 sequences or from MISR triplets.

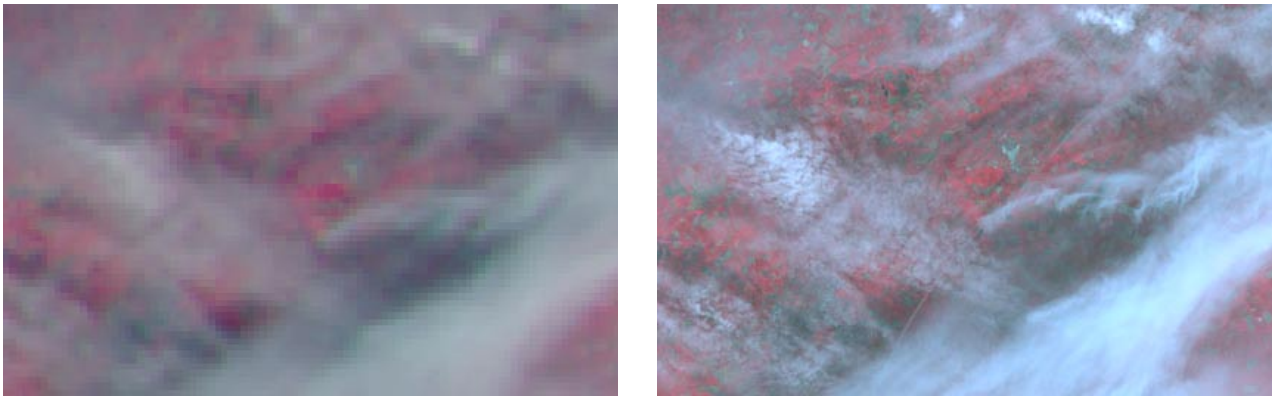

Figure 3. Illustration of the high-resolution cloud structures which are visible in the ASTER image (right) versus the MISR image (left).

Table 3 summarizes the cloud motion results from ASTER, two views of MISR (AN_AF), three views of MISR (BF_AN_DF) und Meteosat-6. The results of Meteosat-6 were resampled to the MISR/ASTER along-/cross-track grid after tracking. The standard deviation of the results over an area with rather constant cloud structures (see Figure 4) is on the same order of magnitude as the theoretical accuracies given in Table 1. The along-track motion accuracy of the MISR triplet BF_AN_DF is slightly worse than the estimated value. It clearly illustrates the problem of the simultaneous CTH/CTW retrieval from MISR triplets for individual cloud points. In Figure 4, these MISR cloud motion vectors are plotted over the BF cloud image, color-coded according to the calculated height value.

Sensor	**Cross-track motion u' [m/s]**	**Along-track motion v' [m/s]**
ASTER	0.9 ± 0.6	-
MISR AN_AF	2.9 ± 1.2	-
MISR BF_AN_DF	2.6 ± 1.8	9.1 ± 7.7
Meteosat-6	0.7	13.9

Table 3. Cloud motion results from ASTER, MISR AN_AF, MISR BF_AN_DF and Meteosat-6 Rapid Scans.

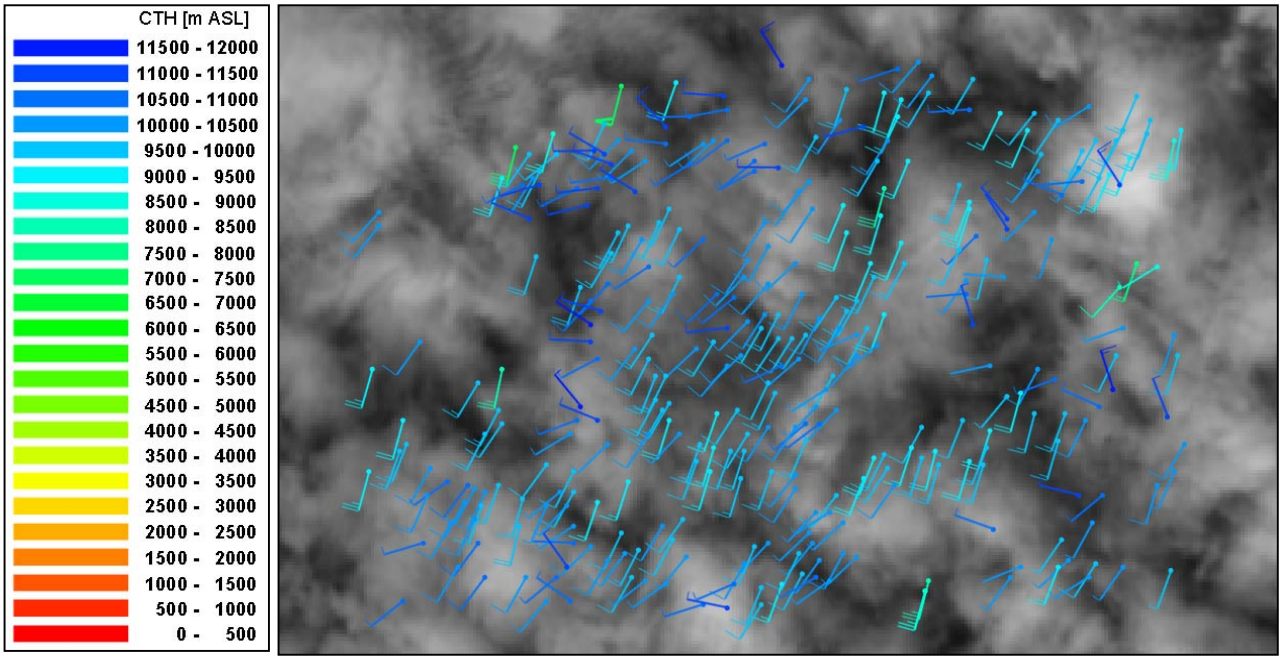

Figure 4. MISR CTH and CTW results from BN_AN_DF triplets. The wind vectors are color-coded according to their CTH value. The wind barbs are drawn in m/s: pennant = 50 m/s, long line = 10 m/s, short line = 5 m/s.

Blunders (if not eliminated in the matching quality control) from either BF-AN or BF-DF matching are then visible either as CTH outliers with too large or too small along-track CTW (e.g. green vector with CTW > 50 m/s) or CTW outliers. Detection of CTH and CTW outliers is relatively easy for one-layer cloud situations where the CTH and CTW fields can be assumed to be continuous. For multi-layer clouds, individual vectors may be derived from different cloud layers, so a successful quality control of the vectors is more difficult to implement.
Stereo CTH on a 1.1 x 1.1 km grid and CTW on a 70.4 x 70.4 km grid are also provided within the operational MISR processing chain as part of the level 2TC product. The algorithms applied for the CTH and CTW retrieval are described in Diner et al. (1999). Important to note is that, due to processing time constraints, no subpixel matching algorithm is used. The L2TC results are not retrieved simultaneously, but in two steps: 1) triplet retrieval of 1-2 CTW values which are representative for the CTW within a 70.4 x 70.4 km box (i.e. first and second peak in histogram) and 2) preliminary CTH retrieval from AN-AF stereo pair for each 275 x 275 m pixel, averaging of the results to the 1.1 x 1.1 km grid and finally correction of these preliminary CTHs with the CTW box values from step 1. The advantage of the L2TC algorithm is the use of a histogram analysis over several hundred triplet matches within each 70.4 x 70.4 km box, which allows to retrieve a rather consistent CTW field at this resolution. The grid resolution could also be increased, e.g. to 37.2 x 37.2 km, as was shown in Horvath et al. (2002). However, the disadvantage of this method is the use of the coarse boxes for the CTW retrieval, which usually introduces artificial discontinuities in the high-resolution CTH field at grid borders. Prior segmentation of the cloud structures would be a promising alternative, allowing both a histogram analysis to reduce the standard deviation of the along-track wind component and a more consistent CTH correction.

5. CONCLUSIONS

In this paper, we have shown the possibilities of high-resolution height and motion retrieval from MISR, ASTER and Meteosat-6. Thereby, the unique combination of two multi-view sensors, ASTER and MISR, on the same satellite platform was highlighted. Multi-view sensors as MISR have a large potential due to the possibility to simultaneously derive CTH and CTW, as we presented with the individual triplet results from the BF-AN-DF view combination. However, the mathematical separability of cloud height and the along-track motion component is not optimal, resulting in a theoretical accuracy of the along-track motion component of only 5-6 m/s, even with a relatively high matching accuracy on clouds of $\pm$ 0.5 pixels. Therefore, correction of preliminary stereo CTHs with the cloud motion retrieved from Meteosat-6 Rapid Scans, with an accuracy of about 3 m/s, is currently still the most accurate solution. With a prior cloud segmentation and histogram analysis, the MISR retrieval could probably be improved substantially. We will in this context also investigate the use of more than 3 views and the introduction of further unknowns (e.g. CTH changes, vertical motion component) into the linear equation system in the near future.
The MSG data offer a new possibility for the stereo CTH correction and CTW comparison. Furthermore, as height assignment of the geostationary cloud winds is still an ongoing research topic, the high-resolution stereo CTHs from ASTER and MISR provide valuable validation data for selected local validation case studies.

ACKNOWLEDGEMENTS

The Meteosat-6 Rapid Scan data were received from the EUMETSAT MARF Archive Facility, the EOS-Terra MISR data (level 1B2 and level 2TC) were obtained from the NASA Langley Research Center Atmospheric Sciences Data Center and the ASTER data were received from the Japanese ASTER User Service. We thank Catherine Moroney, Akos Horvath and Roger Davies, JPL/ University of Arizona, for the reprocessing of the MISR L2TC dataset and for valuable input in the understanding of the L2TC products, Chris Hansen, EUMETSAT, for answers about the Meteosat-6 data, and the ASTER project team that the acquisition from ASTER succeeded in coincidence with our ground measurements. This work is funded by the Bundesamt für Bildung und Wissenschaft (BBW) within the EU-project CLOUDMAP2 (BBW Nr. 00.0355-1).

REFERENCES

ASTER (2003). ASTER homepage at JPL. http://asterweb.jpl.nasa.gov/ (accessed September 25, 2003).

BALTSAVIAS, E.P. (1991). Multiphoto Geometrically Constrained Matching. Ph.D. dissertation, Institute of Geodesy and Photogrammetry, ETH Zurich, Mitteilungen No. 49, 221 p.

DE SMET, A. (2002). Operational AMV Products Derived with Meteosat-6 Rapid Scan Data. Proc. 6th International Winds Workshop, Madison, Wisconsin, USA, 7-10 May, Eumetsat publication EUM P35, Eumetsat, Darmstadt, Germany.

DINER, D., DAVIES, R., DI GIROLAMO, L., HORVATH, A., MORONEY, C., MULLER, J.-P., PARADISE, S., WENKERT, D., AND ZONG, J. (1999). MISR Level 2 Cloud Detection and Classification. JPL Technical Report ATBD-MISR-07, Jet Propulsion Lab., California Inst. of Technol., Pasadena, CA, USA, available at http://eospso.gsfc.nasa.gov/eos_homepage/for_scientists/atbd/docs/MISR/atbd-misr-07.pdf (accessed September 25, 2003).

EUMETSAT (2003). http://www.eumetsat.de/ -> Rapid Scan Service (RSS) (accessed September 25, 2003).

FÖRSTNER, W., GÜLCH, E. (1987). A fast operator for detection and precise location of distinct points, corners, and centers of circular features. Proc. ISPRS Intercommission Conf. on Fast Processing of Photogrammetric Data, Interlaken, Switzerland, 2-4 June, pp. 281-305.

GRUEN, A. (1985). Adaptive least squares correlation: a powerful image matching technique. S. Afr. J. of Photogrammetry, Remote Sensing and Cartography, **14**, 3, pp. 175-187.

HORVATH, A., DAVIES, R. (2001). Feasibility and error analysis of cloud motion wind extraction from near-simultaneous multiangle MISR measurements. J. Atmos. Ocean. Technology, **18**, 4, pp. 591-608.

HORVATH, A., DAVIES, R., SEIZ, G. (2002). Status of MISR cloud-motion wind product. Proc. 6th International Winds Workshop, Madison, Wisconsin, USA, 7-10 May, Eumetsat publication EUM P35, Eumetsat, Darmstadt, Germany.

KEY, J.R., SANTEK, D., VELDEN, C.S., BORMANN, N., THEPAUT, J.-N., RIISHOJGAARD, L.P., ZHU, Y., MENZEL, W.P. (2003). Cloud-drift and water vapor winds in the polar regions from MODIS. IEEE Trans. Geosc. Rem. Sens., **41**, 2, pp. 482-492.

LEWICKI, S., CHAFIN, B., CREAN, K., GLUCK, S., MILLER, K., AND PARADISE, S. (1999). MISR data products specifications. Technical report, NASA JPL, http://eosweb.larc.nasa.gov/PRODOCS/misr/readme/dps_ne_icd.pdf (accessed September 25, 2003).

MISR (2003). MISR Homepage at JPL. http://www-misr.jpl.nasa.gov/ (accessed September 25, 2003).

PRATA, A.J., TURNER, P.J. (1997). Cloud-top height determination using ATSR data. Rem. Sens. Env., **59**, 1, pp. 1-13.

RATTENBORG, 2000. Operational Meteosat Wind Products Towards MSG. Proc. 5th International Winds Workshop, Lorne, Australia, 28 February – 3 March, Eumetsat publication EUM P28, Eumetsat, Darmstadt, Germany.

SCHMETZ, J., HOLMLUND, K., HOFFMAN, J., STRAUSS, B., MASON, B., GAERTNER, V., KOCH, A., VAN DE BERG, L. (1993). Operational cloud-motion winds from Meteosat infrared images. J. Appl. Met., **32**, 7, pp. 1206-1225.

SEIZ, G., BALTSAVIAS, E.P. (2000). Satellite- and ground-based stereo analysis of clouds during MAP. EUMETSAT Conference Proceedings, Bologna, pp. 805-812.

SEIZ, G., BALTSAVIAS, E.P., GRUEN, A. (2001). Comparison of satellite-based cloud-top height and wind from MISR, ATSR2 and Meteosat-6 Rapid Scans. EUMETSAT Users' Conference, Antalya, 1-5 October 2001. EUMETSAT Conference Proceedings, pp. 224-230.

SEIZ, G. (2003). Ground- and satellite-based multi-view photogrammetric determination of 3D cloud geometry. Ph.D. thesis, Institute of Geodesy and Photogrammetry, ETH Zuerich, June 2003. IGP Mitteilungen Nr. 80.

WALLIS, R. (1976). An approach to the space variant restoration and enhancement of images. Proc. of Symp. on Current Mathematical Problems in Image Science, Naval Postgraduate School, Monterey CA, USA, November.